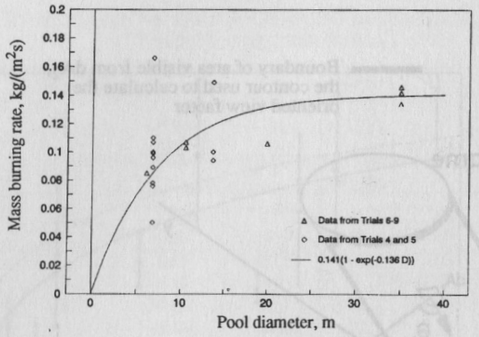

FIG. 2 - Mass burning rate correlation

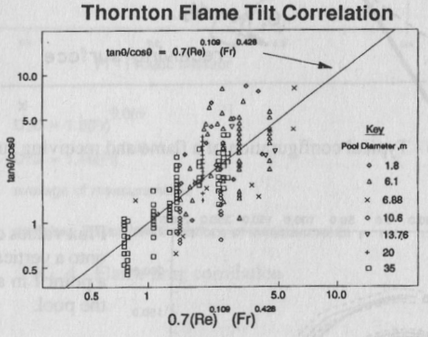

FIG.3(a)

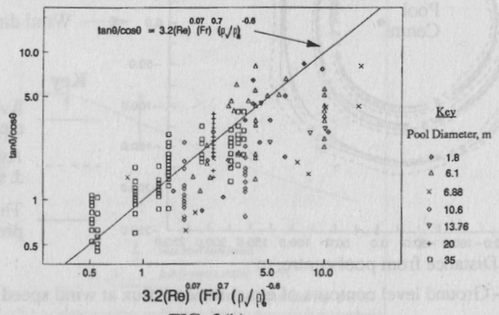

FIG. 3(b)

FIG. 3 - Flame tilt correlation

SPHERICAL EXPLOSIONS AGGRAVATED BY OBSTACLES

H. Phylaktou, G.E Andrews, N. Mounter and K.M. Khamis
Department of Fuel and Energy, The University of Leeds, Leeds LS2 9JT

There is very little data in the literature on the quantitative effect of obstacles on explosions. This leads to an uncertainty when designing explosion protection measures for obstacle congested volumes. In this work the effect of high-blockage, spherical-grid obstacles was investigated in an enclosure of 0.5 m in diameter and 0.5m in length. Methane, Propane, Ethylene and Hydrogen were used as explosive mixtures with air. Turbulence enhancement factors up to 15 were measured with an 80% blockage. A model based on turbulence generation and turbulent combustion was developed and this predicted turbulence factors in good agreement with the experimental results. It also predicted a weak dependence on the type of gas/air mixture and a strong dependence on the obstacle geometry. Both of these predictions were supported by the experimental results.

Key Words: Spherical Explosions, Obstacles, Turbulence Factor, Model.

INTRODUCTION

In the deflagration of a flowing gaseous mixture the flow characteristics are an integral part of the combustion process. Even if the combustible gas is initially stagnant, the expansion of the hot burnt gases behind the flame front will set up a flow in the unburnt gas ahead of the flame and this flow in turn, may stretch and fold the flame, produce turbulence and initiate instabilities. All these phenomena contribute to the enhancement of thecombustion rate. This enhancement can be further augmented by particular shapes of the explosion geometry or by the presence of obstructions in the path of the flame.

In explosions, the combustion sets up a gas flow which acts as positive feedback loop on the combustion itself (1). This coupling mechanism between flame acceleration and gas flow dynamics is the key problem in gas explosions, whether confined or unconfined. The strength of the feedback loop, and the flame acceleration can be very extreme in the presence of turbulence generating obstacles. This was demonstrated by Phylaktou and Andrews (2,3) in gas explosions in long vessels with one or two orifice-plate type obstacles in the path of the propagating flame, where the combustion rate was measured to increase by a factor of up-to 200, compared to the unobstructed explosion. While such an effect would be considered as a beneficial enhancement in a controlled combustion process, and indeed turbulent burning is the normal mode of operation in many combustion systems, it can not be considered as an 'enhancement' in an accidental explosion scenario. Obstacles have rather an aggravating effect on an explosion; they

make a dangerous situation potentially more damaging and result in increased protection-measure requirements.

Many practical volumes and enclosures where an explosion hazard exists are likely to contain obstructions in various forms. The majority of experimental data on vented (or unvented) explosions on which the current methods for venting are based (4,5,6), has been obtained under conditions of low turbulence in simple geometries. Lunn (7) underlined the failure of empirical, semi-empirical and theoretical methods to adequately consider the effects of turbulent combustion and obstacles. In current practice, the influence of these obstacles is allowed for by the introduction of a turbulence factor (β). Essentially, this is done by using a value of turbulent burning velocity, S_T, in the equations, related to the maximum laminar value, S_L, by:

$$S_T = \beta \cdot S_L \qquad (1)$$

The problem, however, is that there exists no design procedure for the evaluation of the numerical factor β. Although some values for β are suggested by Rasbash et al (4) experimentally determined values are sparse. Harris (8) concluded that evaluating β has to be subjective, and other explosion venting guides such as the NFPA 68 (9) recognise that there is insufficient information to give detailed venting guidelines when obstacles are present.

Rasbash et al (4) in their recommendations for the design of an explosion relief system for enclosures of room or laboratory size, suggested a factor of 1.5 for the turbulence generated by furniture and other obstacles restricted mostly to one level. For situations in which an explosion (of an initially quiescent combustible mixture) propagates through large openings into other sections of the enclosure (e.g. propagation from one room to another through an open door), or where obstacles are distributed throughout the entire volume of the enclosure they quote a value of β=5. In more severe cases of turbulence, for example one combining high pressure leakage of fuel and an obstacle congested enclosure, they recommend that a more appropriate value of the turbulence factor would be 8 or 10.

Dorge et al (10) carried out a more methodical investigation of the influence of spherical wire mesh screens on the flame propagation speeds of essentially unconfined gas explosions. The mixture was ignited at the centre of the spherical screen and measurements were made (using streak photography) of the flame propagation speeds inside and outside the screen. The turbulence factor was equated to the ratio of the flame speed outside to that inside the grid. They varied the screen diameter, the mesh size and wire diameter, the blockage ratio (20-75%), the number of concentric screens (1-3) and the mixture reactivity. With a single screen the maximum turbulence factor they obtained was 5 while with three screens and acetylene/air mixtures the the turbulence factor was 12. With oxygen enriched mixtures detonation was sometimes obtained.

The present work is similar to the above investigation with the difference that perforated, spherical, thin shells were used as obstacles which produced turbulence with a larger length scale than that of wire mesh screens used by the previous workers. We will show that a single obstacle of

this kind produces significantly higher turbulence factors than those reported above and it will be demonstrated that these factors can be predicted from turbulence- generation and turbulent combustion considerations. Effectively, a model will be presented that could be used to quantify the turbulence factor β for geometries of this type.

EXPERIMENTAL

The explosion geometry was a totally confined cylindrical vessel, 0.5m long and 0.5m in diameter, made of mild steel. It was designed to operate at 25 bar in anticipation of possible detonation pressures being generated due to the influence of the obstacles. The one-atmosphere pressure gas/air mixture was formed by partial pressures and a homogeneous composition was achieved by circulating the gases in the vessel using an external recirculation pump. The mixture was allowed to rest and then it was ignited at the centre of the vessel by means of a 16-joule-strong spark-discharge. A schematic presentation of the experimental set-up is given in Fig.1.

The obstacles used were hollow stainless steel spheres, 203mm in diameter and 1mm shell thickness. These are commercially available as water-tank ball-floats.They were mounted in the centre of the vessel with sphere and vessel centre coinciding with the sparking point.

Blockage Ratio	No of Holes	Hole Diameter mm
0.6	4	122
0.6	12	73
0.6	20	56.9
0.8	32	31

Table 1. Spherical obstacle characteristics

They were modified for our purposes by cutting out equal size holes on the surface to provide the required blockage ratio (BR) - defined as the ratio of blocked area to the total surface area of the sphere. Care was taken so that the holes were evenly distributed over the whole surface of the obstacle. To achieve this, spherical trigonometry and geometry of regular polyhedra was employed where appropriate. A collective summary of the relevant dimensions of the obstacles tested is given on Table 1.

The flame travel was recorded by an array of mineral insulated, exposed junction, type K thermocouples. The time of flame arrival was detected as a distinct change in the gradient of the analogue output of the thermocouple and from this the average flame speed between any two thermocouples could be calculated. The thermocouples were positioned radially and when the obstacles were present, they were on the centreline of one of the obstacle holes. This method of measuring the flame speed has been compared with high

speed photographic measurements in spherical flame explosions and has been shown to give excellent agreement (11). The pressure variation was recorded by a SENSYM pressure transducer mounted at the top flange.

A 16-channel (1MHz) transient data recorder (AIMS - Computerscope) was used to capture the data. A signal conditioning and processing package (FAMOS) was used to process the pressure signals. Mixtures of methane, propane, ethylene and hydrogen with air were tested at concentrations of 10, 4.5, 7.5 and 40% (v/v) respectively. At these concentrations the maximum combustion rates were produced for each gas. Each explosion was repeated at least 3 times and averaged readings were used.

EXPLOSIONS WITH SPHERICAL OBSTACLES

The expansion of the burnt gases inside a spherically propagating flame-front induced a flow in the unburnt gases ahead of the flame. In the presence of a perforated spherical obstacle, the unburnt gas-flow was forced through the obstacle holes and generated turbulence downstream of the baffle. When the flame encountered this turbulence the combustion rate was increased and this was detected as an acceleration of the flame speed and an increase in the rate of pressure build-up in the vessel.

Typical pressure-time profiles with and without the 80% blockage are shown in Fig.2a for a 10% methane/air mixture. The early rapid increase in pressure in the obstructed explosion was due to the turbulent combustion in the near-region downstream of the obstacle. As a result, the explosion duration was about half of that without the obstacle. Considering that a typical vent opening over-pressure might be 300 mbar it can be seen that at the time this pressure is reached, the rate of pressure increase is a lot higher in the obstructed explosion. The rate of pressure increase (dP/dt) is an important parameter in the design of vents or suppression systems because for successful containment the pressure has to be relieved or suppressed at a rate equal to its generation rate. This has a direct implication on the size of the vent (or amount of suppressant) required. Therefore the ratio of the rate of pressure rise with the baffle to that without the baffle would provide the factor of vent-area increase needed for the venting process to cope with the effect of the obstacle. In summary the effect of the obstacle is twofold; it results in reaching dangerous over-pressures earlier and the rate of pressure generation at the danger level is much faster. This means that explosion mitigation devices will need to activate and respond much earlier in the explosion and will need to suppress or relieve the pressure at a faster rate. How much earlier will depend on the distance between the ignition point and the obstacle and how much faster will depend on the turbulence factor associated with the obstacle geometry and the prevailing flow conditions.

Phylaktou and Andrews (2) have demonstrated that the normalised rate of pressure rise (defined as the rate of pressure rise with the obstacle to that without the obstacle) is equal to the turbulence factor β and this method was employed here to quantify β experimentally. However, the increase in dP/dt due to the presence of the obstacle was not easy to measure directly from the raw pressure signals and it was strongly dependent on the judgment of the investigator as to where exactly the maximum effect of the obstacle was. In

order to eliminate the subjectiveness of the process and ease the measurement of dP/dt, the pressure signals were smoothed and then differentiated to produce dP/dt curves versus time, as shown in Fig.2b. Smoothing of the pressure record was necessary in order to remove noise and high frequency pressure oscillations which would otherwise dominate the differentiated signal. Particular care was taken not to "over-smooth".

The dP/dt for the unobstructed explosion (Fig.2b) showed a gradual increase associated with the increase in the flame area and hence the increase in the combustion rate as the explosion propagated spherically away from the ignition point. It reached a maximum value when the flame area was at its maximum i.e. just before it was quenched on the vessel walls. It then decreased rapidly as combustion was completed in the corners of the vessel. When the obstacle was present the rate of pressure showed two maxima points marked A and B in Fig.2b. The maximum value at A was due to the presence of the obstacle. The rate of pressure rise begun to rise sharply at the wake of the obstacle and reached a maximum value at A, some distance downstream of the obstacle and then begun to decay. This profile of dP/dt downstream of the obstacle agrees with the expected turbulence-intensity profile for the same region, as it will be discussed later. The second rise in dP/dt and maximum at B was equivalent to that observed for the explosion without the obstacle i.e. due to the large flame area just before reaching the vessel walls. The fact that the actual maximum value of dP/dt at B was equal to that of the explosion without the obstacle indicated that the effect of the obstacle did not extend as far as the near-wall region of the vessel. The decay in the rate of pressure after the peak A in the explosion with the obstacle demonstrated quite clearly that at some point between the obstacle and the wall the influence of the obstacle started to decrease very rapidly.

In order to quantify the effect of the obstacle, the maximum rate of pressure rise induced by the obstacle (i.e. as measured at A) was divided by the corresponding rate without an obstacle. This normalisation of dP/dt produced a factor which has been shown (2) to be equal to the turbulence factor β defined by Eq.1.

Another way of obtaining a measure of the turbulence factor is by dividing the maximum flame speed induced downstream of the obstacle to that without the obstacle in place. The flame speed as a function of the flame radius is shown in Fig.3 for three of the gases used for explosions with an 80% blockage. It should be noted that these are the flame speeds as recorded on the centreline of the obstacle holes. In agreement with the dP/dt profile the flame accelerates downstream of the obstacle reaches a maximum value within 50mm and then rapidly decays. The ratio of the maximum flame speed with the obstacle to that without-it gives a factor comparable to but lower than the value obtained from normalising the rates of pressure rise, as described earlier. For example the ratio of flame speeds for the ethylene explosion was 10 while the normalised rate of pressure rise was 14.2 for the 80% blockage. It was felt that the normalised rates of pressure provided a more accurate value of the turbulence factor because:

a. dP/dt represents a more accurate overall measure of the rate of burning, while the flame speed measured in one direction might be different in another,
b. there were more errors involved in the measurement of flame speed (exact distance between thermocouples, timing of flame arrival etc),
c. the flame speed record was discontinuous and of low resolution.

For these reasons the experimental turbulence factors reported in this presentation are based on the normalised dP/dt. Dorge et al (10) employed the flame speed approach -and this was more appropriate in their set up- because their tests were not contained in a closed vessel and using photography they were able to obtain a continuous record of the flame movement.

Pressure oscillations were present towards the end of the combustion, in all the laminar explosions, except for those of methane. With the obstacle in place these oscillations appeared more readily and were stronger as the reactivity of the gas was increased. Figure 4 shows an example of the 40% Hydrogen/air explosions with and without the obstacle. With the obstacle these oscillations were triggered by the flame interaction with the baffle. A particular feature of all the constricted hydrogen explosions was the large pressure spike at the position of maximum turbulence intensity, as shown in Fig.4. At this point the estimated flame speed (based on the measured turbulence factor) was in excess of 300m/s and it is possible that, what was observed was a short lived pseudo-detonation. Dorge et al (10) reported detonation in their unconfined experiments when they used multiple screens with oxygen-enriched mixtures whose laminar burning velocity exceeded 2 m/s.

A SIMPLIFIED PREDICTIVE MODEL

Turbulent Combustion

The progress in understanding turbulence and turbulent combustion mechanisms has been slow, despite the continuous interest that the subject has been receiving. Today we are still far from a universal model that would satisfactorily explain the turbulent premixed flame data available in the literature. The literature on turbulent combustion is both vast and diverse and is not proposed to be reviewed in detail here.

A simple equation relating the turbulent burning velocity (S_T) to the laminar burning velocity (S_L) and the rms fluctuating velocity of the flow field (u') has been proposed by a number of researchers and has the form of

$$S_T/S_L = 1 + C\, u'/S_L \qquad (2)$$

where C is a constant. This model was originally proposed by Damkohler (12) with the value of the constant equal to 1. The intercept of 1 in the above equation arises from the need to satisfy the boundary condition that as $u' \to 0$ then $S_T \to S_L$. Equation 2, or similar - with sometimes a different value for C, and/or with the right hand side to some power - has been proposed by a number of subsequent researchers detailed in the reviews by Andrews et al (13) and Gulder (14). Equation 2 and all of its variations in the literature shows that the turbulent burning velocity (S_T) is only dependent on u' and S_L. Furthermore, at high turbulence levels where $u' \gg S_L$ (which is the case in most practical systems), S_T becomes a function of u' only. It is

interesting that in this model of turbulent combustion the turbulent burning velocity is independent of the characteristic length scale of turbulence. Even in the formulations where an influence of the length-scale is predicted this is indicated to be small.

The reported value of the constant C in Eq.2 is widely varied, and in an attempt to obtain a large-sample average of this constant a number of data sets from the literature were combined and plotted in terms of the variables in Eq.2, as shown in Fig. 5. The plot contains 769 points from 25 publications. These data, with the exception of those of Al-Dabbagh and Andrews (15) and Abdel-Gayed et al (16), were collected and reported by Andrews et al (17) as the ratio of burning velocities (S_T/S_L) against the turbulent Reynolds number based on the Taylor microscale (R_λ), and were subsequently used by Bradley and co-workers in the development of their models.

For full details of the sources and method of interpretation of the data in Fig.5 the reader is reffered to the papers by Andrews et al (17) and Abdel-Gayed and Bradley (18). The data by Al-Dabbagh and Andrews (15) in Fig.5 were obtained with weak premixed propane/air flames stabilised on grid plate geometries at simulated gas turbine conditions. Weak extinction was postulated to occur when the mean flow velocity exceeded the turbulent burning velocity and this was used to measure S_T. The intensity of turbulence was determined from empirical correlations of grid generated turbulence; these calculations were corrected by bettter relationships based a larger number of experimental data on grid generated turbulence - developed as part of the present project to be presented in later sections. The data of Abdel-Gayed et al (16) were obtained in a an explosion bomb with fan induced turbulence. The data of Petrov and Talantov (19) are highlighted in Fig.5 because they were considered to be too low by Abdel-Gayed and Bradley (18) while the data of Kozachenko (20-22) and Kozanchenko and Kuznetsov (23) were thought to be too high and the data of Khitrin and Goldenberg (24) were not considered at all by Bradley's group (16,18,25).

The data scatter in Fig.5.1 is considerable and it is somewhat disguised by the log-log plot. The experimental data cover many fuels and equivalence ratios and have been obtained on a variety of rigs by different researchers. There are significant errors associated whith the measurement of the relevent variables, or with their estimation in the cases that they were not measured by the original researchers. For example, there are errors associated with the experimental measurement of the laminar burning velocity and these are even greater when determining the turbulent burning velocity. Measurements of the integral length scale of turbulence are difficult to make and although accurate measurements of the rms turbulent velocity can usually be made these were done under cold flow conditions (no combustion) or not done at all - in which cases approximate estimates were used (18).

Nevertheless, despite these difficulties, Fig.5 shows that Eq.2 describes reasonably well the relationship between the plotted variables. The correlation coefficient between S_T/S_L and u'/S_L was calculated to be 0.78, which means that 78% of the variation in S_T/S_L could be accounted-for by a linear relationship with u'/S_L. The average value of the constant C was found to be equal to 2.03, and so Eq.2 becomes

$$S_T/S_L = 1 + 2.0\ (u'/S_L) \qquad (3)$$

This equation is shown as a solid line going through the bulk of the experimental data in Fig.5. The value of 2.0 of the constant C is supported mainly by a large number of Kozachenko's and Al-Dabbagh & Andrews' data. Strong support for this value of C comes also from some theoretical models. Magnussen (26) in his eddy dissipation theory that takes into account the intermittent influence of the small scale structures on the chemical reactions and alllows for both fast and slow chemical reactions to be treated simultaneously, predicted that for typical shear flow situations the turbulent flame propagation velocity is given by $S_T = 2u'$ which is similar to Eq.3 since at high values of u' the influence of S_L in this equation becomes negligible. An almost identical equation ($S_T = 2.1\ u'$) was reached by Pope and Anand (27), on the basis of their analytical solution of a transport equation for the joint probability density funcion of velocity and the progress variable by a Monte Carlo method (in the wrinkled flame regime).

In summary, there is strong evidence in the literature that the ratio S_T/S_L is linearly dependent on u'/S_L only. A large sample of experimental data indicated that the average value of the proportionality constant is 2.0 as indicated by the solid line in Fig.5, and this is supported by some theoretical models. The data scatter was considerable and although most of the data could be enveloped within the broken lines which correspond to values of the constant C in Eq.2 of 0.5 and 4.0 as shown in Fig.5, at the extremes C varied from near 0.0 to 20. Equation 3 is therefore an approximate practical correlation of turbulent combustion parameters that can be used for the calculation of the turbulent burning velocity S_T. However, before this equation can be applied, a value of the rms turbulent velocity (u') is required, which is dependent upon the flow velocity and the turbulence generation characteristics of the constriction..

Turbulence Generation

The pressure drop ΔP in the flow across a constriction is characteristic of the geometry of the constriction and is usually expressed in a non-dimensional form as either the discharge coefficient C_d or the pressure loss coefficient K. The latter is defined by the following equation:

$$K = \frac{\Delta P}{\frac{1}{2}\rho U^2} \qquad (4)$$

where ρ is the density of the fluid and U is the mean velocity of the flow. The pressure energy loss must appear as turbulence energy prior to dissipation as molecular motion and therefore ΔP can be equated to the turbulent kinetic energy as in Eq.5 (15).

$$\Delta P = \frac{3}{2}\rho u'^2 \qquad (5)$$

Combining Eqs. 4 and 5 produces an equation for the turbulence intensity given by:

$$u'/U = C K^{0.5} \qquad (6)$$

where C is a constant, equal to 0.58 in theory but in practice must be less than that because not all pressure loss through a constriction is translated to turbulent, isotropic, kinetic energy.

Grid induced turbulence has been used for fundamental studies of turbulence (28), but most measurements have been made well downstream of the grid-plate in the turbulent decay period, where the turbulence is isotropic. Maximum turbulence occurs at the end of the potential core region of the jets produced by the grid-plate. Measurements of the turbulence intensity, u'/U, in the region immediately downstream of the grid have been carried out by Baines and Peterson (29), Robinson and Covitz (30), and Checkel (31), in cold-flow, wind tunnel experiments. An example of these near grid measurements of turbulence is reproduced in Fig.6 from the work of Baines and Peterson (29). It is shown that the turbulence intensity begins to increase immediately downstream of the grid, it reaches a maximum value some distance after it, and it then begins to decay at a more or less steady rate over a relatively long distance..

In order to obtain a practical value C in Eq.6, the maximum turbulence intensity as measured by the above workers was correlated to the pressure loss coefficient K of the grid employed, as shown in Fig.7. The turbulence intensity was found to be proportional to the square root of K, as predicted by Eq.6, and the results were found to fall on two lines depending on the thickness to diameter ratio (t/d) of the orifice. The influence of t/d on the flow characteristics through an orifice has been investigated, amongst others by Ward Smith (32), who showed that for t/d above a critical range reattachment of the flow to the orifice walls occurs. This reduces the baffle pressure loss characteristics and therefore there is less energy available for the creation of turbulence downstream the baffle. This is illustrated in Fig.7 where it is shown that thicker baffles create lower turbulence intensities for the same K.

The equations of the fitted lines showing the trend of the data in Fig.7 are as follows:

For thin baffles ($t/d < 0.6$):

$$(u'/U)_{max} = 0.19\ K^{0.5} \qquad (7)$$

For thick baffles ($t/d > 1$):

$$(u'/U)_{max} = 0.07\ K^{0.5} \qquad (8)$$

These equations enable the maximum turbulence intensity generated by a grid-like obstacle to be estimated from simple knowledge of its pressure loss characteristics. Ward Smith (32) correlated a large number of experimental pressure loss coefficient measurements to the geometry of the constriction.

His proposed equations are:

$$K=\left[\frac{1}{0.608p(1-p^{2.6})(1+(t/d)^{3.5})+p^{3.6}}-1\right]^2 \qquad (9)$$

for data in the ranges

$$0 < t/d < 0.6, \quad 0 < p < 0.75, \quad 0.57 < K < 35000$$

and

$$K=\left[\frac{1}{p(.872-.015t/d-.08d/t)(1-p^{3.3})+p^{4.3}(1+.134(t/d)^{.5})^{-1}}-1\right]^2 \qquad (10)$$

for data in the ranges

$$0.98 < t/d < 7.1, \quad 0 < p < 0.48, \quad 2.4 < K < 63400$$

where p is the porosity (= 1 - BR).

Combining Eqs. 1,3 and 6 gives an equation for the turbulence factor β based on the maximum turbulence intensity, as

$$\beta = 1 + 2\ C\ U\ K^{0.5}/S_L \qquad (11)$$

U in Eq.11 is the flow velocity which in initially quiescent explosions is equal to the unburnt gas velocity S_g induced by the flame propagation. In a spherical explosion S_g is given by:

$$S_g = S_f - S_L \qquad (12)$$

where S_f is the flame speed. This was measured for the different gas/air mixtures in our experimental set- up without the obstacle in position. The average of a large number of measurements of S_f at the obstacle position gave values of 2.63 m/s for methane, 2.88 m/s for propane, 5.97 m/s for ethylene and and 24.03 m/s for hydrogen. Standard S_L values were used (ie 0.45, 0.53, 0.83 and 3.5 m/s for the above gases respectively).

Substituting Eq.12 into 11 gives:

$$\beta = 1 + 2\ C\ (S_f - S_L)\ K^{0.5}/S_L \qquad (13)$$

The constant C is equal to 0.19 or 0.07 from Eqs. 7 and 8 and K was calculated from either Eq.9 or 10. It should be noted that we did not adhere strictly to the porosity ranges of Eqs. 9 and 10. Both equations were applied to all values of p between 0.1 and 0.9.

PREDICTIONS AND EXPERIMENTAL RESULTS

The predictions for the turbulence factor β over the range of 10 to 90% blockage ratio are shown in Fig.8 for the different gas/air mixtures tested experimentally, and for both thin and thick type of obstacles. Our experimental measurements of β as well as those of Dorge et al (10) are also included in Fig.8 for comparison with the predictions.

In general there was good agreement between the predictions and the experiments, considering the uncertainty in some of the equations used for the prediction model, Eq.3 in particular. In all of our experimental results the aspect ratio (t/d) of the obstacles was small and so these results should fall on the prediction lines for thin or sharp-edge obstacles. The measurements at the 80% blockage ratio gave good agreement with the predictions while those at 60% fell below the predictions. The obstacles at 60% BR had different number of holes on their surface -in an attempt to get an indication of the effect of the turbulence length scale. The 20 hole sphere gave higher β factors than the 12 hole which gave higher values than the 4 hole one. By decreasing the number of holes the turbulence length scale (which in grid-type obstacles is associated with the distance between the edges of the holes) is increased, which usually results in higher turbulence levels. However, in the present arrangement the 20 hole sphere gave a much better distribution of the turbulence, which is possibly why it produced higher β factors.

The experiments of Dorge et al (10) were with round-wire meshes and any constriction with a rounded profile has a discharge coefficient of 1 and therefore their results should agree with the predictions for "thick or rounded-edge" obstacles in Fig.8. Most of the data agreed with or was just above the predicted values. The ethylene data of Dorge et al (10) at 30% blockage which fell on the prediction lines for sharp-edge obstacles were obtained with meshes of wire diameter of 0.25 mm. It could be argued that such a wire is a sharp edge and therefore there was agreement with the predictions. Most of the wire meshes with a wire diameter greater than 1mm gave results lying firmly on the model lines for thick or rounded-edge obstacles.

The predictions in Fig.8 showed a very small dependence on the reactivity of the gas/air mixture and this is validated by the experimental results. Another outcome of the predictions (not shown in Fig.8) was that the aspect ratio (t/d) had negligible influence once the obstacle was either in the thin or the thick range.

The current recommendations in the literature for turbulence factors induced by obstructions in compact vessel explosions (based on the empirical suggestions of Rasbash et al (4)) are similar to those measured and predicted for thick obstacles in Fig.8. For thin obstacles with a blockage higher than 60% β is higher than the maximum (of 10) recommended. If the blockage is higher than 85% β factors of the order of 20 to 40 and higher are predicted. Furthermore the present predictions and experiments are for initially quiescent mixtures with single obstacles. It is evident that if the gases are already flowing at the time of ignition or if there repeated layers of obstacles the turbulence factors will be higher than those shown in Fig.8. A programme for investigating experimentally, high-blockage, single

thin obstacles and multiple obstacle situations is currently under way.

The prediction model presented here was originally developed and applied to explosions in long tubes with single and double obstacles (Phylaktou and Andrews 1991a; 1991b) where the flow velocities induced by the explosion are a lot higher than those in spherical explosions. The model successfully predicted the turbulence factors generated under those conditions as well. The β factors were much larger and explosions in large L/D enclossures represent a much more severe situation for the influence of obstacles than the present low L/D work.

CONCLUSIONS

The influence of spherical-grid type obstacles has been investigated in explosions in a 0.5 m diameter compact vessel. The expanding flame front induced a flow of unburnt gas ahead of it and through the holes of the obstacle. This resulted in flow turbulence downstream of the obstacle and when the flame reached this turbulent region the combustion was enhanced resulting in higher flame speeds and rates of pressure rise. This increase in the rate of pressure rise has a direct implication in the design of explosion mitigation measures. A single obstacle with 80% blockage induced a turbulence factor of up to 15 which is higher than current recommendations -which are based on very little data.

By applying current concepts of turbulence generation and turbulent combustion a model has been developed which successfully predicted the measured turbulence factors for different types of obstacles and different gas/air mixtures. The dependence on the gas reactivity was predicted to be small and this was validated by the experimental data. Thin and sharp-edge obstacles were predicted to produce higher turbulence factors than thick or round-edge ones and this was again supported by the experiments.

The proposed model could form a basis for the design of explosion-relief measures for volumes where obstacles are present. Before that, however, further validation of the model is required particularly at high blockage ratios where turbulence factors of the order of 40 are predicted. More experimental data is also required in the low blockage region.

Acknowledgements

We thank the Science and Engineering Research Council for financially supporting this work. Bob Boreham made the spherical baffles and commissioned the test rig.

References

1. Solberg, D. M.,1982, Plant Operation Prog.,1 p.248.
2. Phylaktou H. and Andrews G. E., 1991, Combust. and Flame, 85, p.368
3. Phylaktou H. and Andrews G. E., 1991, Fire and Explosion Hazards, p.63, The Inst. of Energy.
4. Rasbash, D. J., Drysdale, D. D. and Kemp, N., 1976, IChemE Symposium Series No.47.
5. Runes, E., 1972, Loss Prevention, 6, p.63.
6. Bartknecht, W., 1981, Explosions, 2nd Ed., Springer-Verlag.
7. Lunn, G. A., 1984, Venting Gas and Dust Explosions - A Review, An ICHEME Industrial Fellowship Report, The Institution of Chemical Engineers
8. Harris, R. J., 1983, The Investigation and Control of Gas Explosions in Buildings and Heating Plant, E & FN Spon.
9. NFPA 68, 1978, Explosion Venting, National Fire Protection Association Inc.
10. Dorge, K. J., Pangritz, D. and Wagner, H. G., 1976, Acta Astronautica, 3, p 1067.
11. Herath, P. ,1986, Closed Vessel Explosions: The Influence of Baffles, Ph.D. Thesis, The University of Leeds
12. Damkohler, G., 1940, Z. Elektrochemie Angewandre Phys. Chem.,46, p601. (English translation, NACA TM1112 (1947))
13. Andrews, G.E., Bradley, D. and Lwakabamba, S.B., 1975, Cobust. Flame, 24, p.285.
14. Gulder, O. L., 1990, Twenty-Third Symposium (International) on Combustion, p.743, The Combustion Institute.
15. Al-Dabbagh, N. A. and Andrews, G. E., 1984, Combust. Flame, 55, p.31.
16. Abdel-Gayed, R.G., Al-Kishali, K.J. and Bradley, D., 1984, Proc. R. Soc. Lond., A301, p393.
17. Andrews, G.E., Bradley, D. and Lwakabamba S.B., 1974. Fifteenth Symposium (International) on Combustion, p665, The Combustion Institute.
18. Abdel-Gayed, R.G., and Bradley, D., 1981, Proc. R. Soc. Lond. A301,p.1.
19. Petrov, E.A. and Talantov, A.V., 1959, Izv. Vysh. ucheb. Zaved., Aviat. Teknol., 3, p91 (English translation: ARSJ 31, p408 (1961)).
20. Kozachenko, L.S., 1960, The third All-UnionCongress on Combustion Theory, Moscow, Vol.1, p126.
21. Kozachenko, L.S., 1960, Bull. Acad. Sci., USSR, Div. Chem. Sci., No1, p37
22. Kozachenko, L.S., 1962, Eigth Symposium (International) on Combustion, p567, The Combustion Institute.
23. Kozachenko, L.S. and Kuznetsov, I.L., 1965, Comb. Exp. Shock Waves, 1, p.22
24. Khitrin, L. and Goldenberg, S. A. 1962, Gas Dynamics and Combustion (AS Predvoditelev, Ed.) p139, IPST.
25. Abdel-Gayed, R.G., and Bradley, D., 1982, Fuel-air Explosions, p.51. Montreal: University of Waterloo Press.
26. Magnussen, B.,1985, AGARD-CP-390, p.23.
27. Pope, S.B. and Anand, M.S., 1985, Twentieth Syposium (International) on Combustion, p403, The Combustion Institute.
28. Gad-el-Hak, M. and Corrsin, S., 1974, J. Fluid Mech. 62, p115
29. Baines, W.D. and Peterson, E.G., 1951, Trans. ASME, 73, p167
30. Robinson, G.F. and Kovitz, A.A. 1975, AAIA J., 13, p.1488.
31. Checkel, M.D., 1981, Turbulence Enhanced Combustion of Lean Mixtures, Ph.D Thesis, Cambridge University.
32. Ward Smith, A.S., 1971, Pressure Losses in Ducted Flows, London Butterworths.

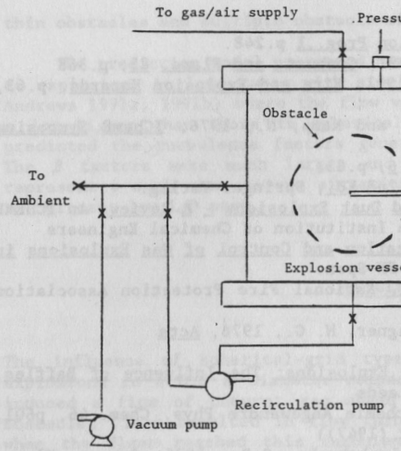

Fig. 1. Experimental set up.

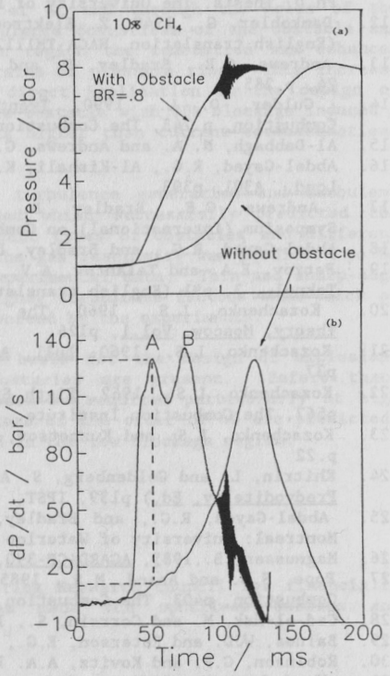

Fig. 2. (a) Typical pressure-time profiles for 10% methane/air explsions with and without an 80% spherical blockage.

(b) The rates of pressure rise as produced by differentiation of the smoothed pressure signals above. The dashed lines indicate the dP/dt values whose ratio gave the experimental turbulence factor.

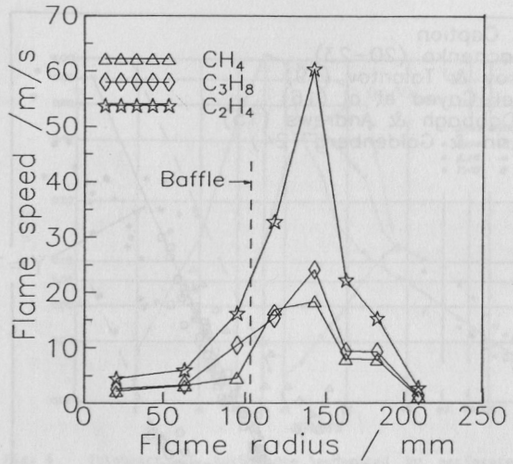

Fig. 3. Flame speeds of three of the test gases as function of the flame radius with an obstacle of 80% BR at 103mm from the spark.

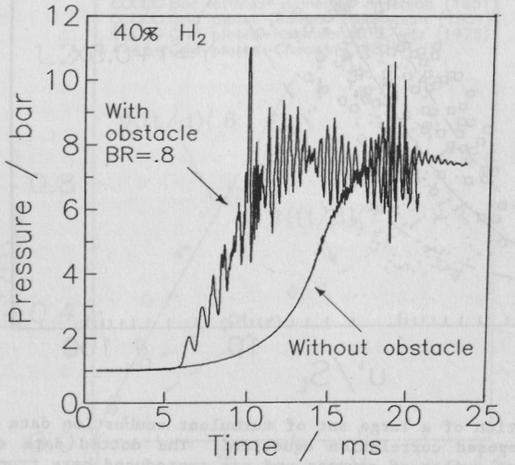

Fig. 4. Typical pressure signals of a 40% hydrogen/ air explosion with and without an obstacle.

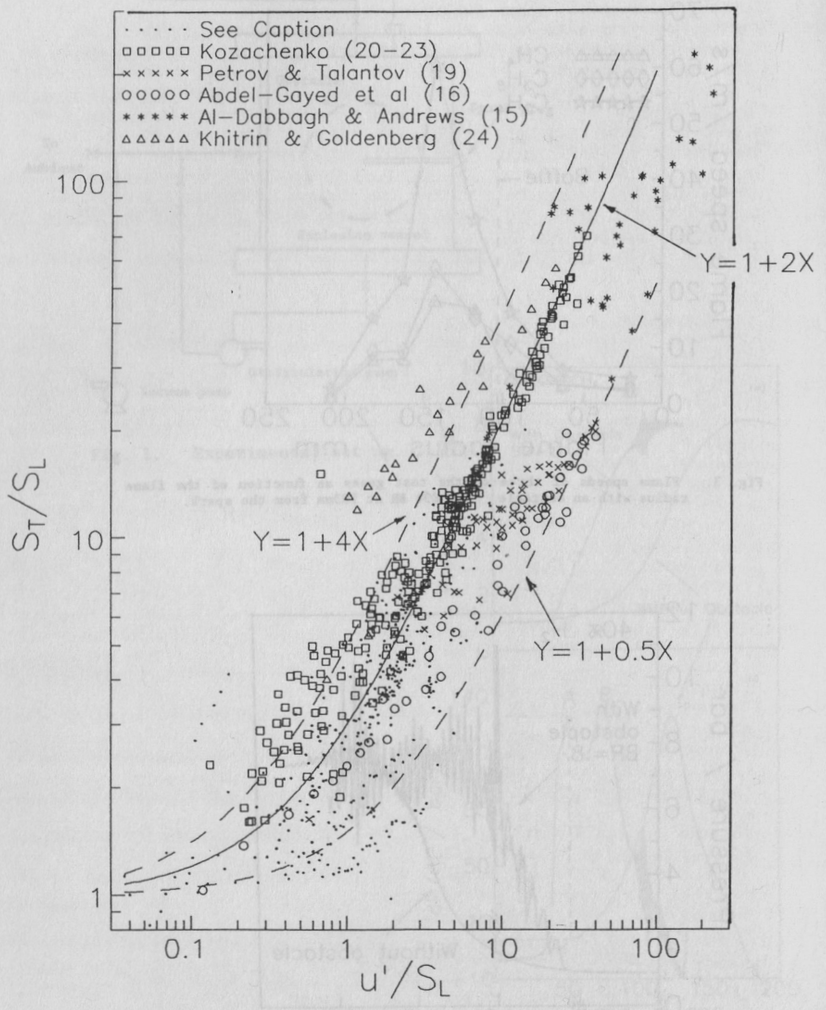

Fig. 5. A compilation of a large set of turbulent combustion data compared to the proposed correlation equation. The dotted data originate from a large number of sources and are reproduced here from Andrews et al (17) and Abdel-Gayed and Bradley (18).

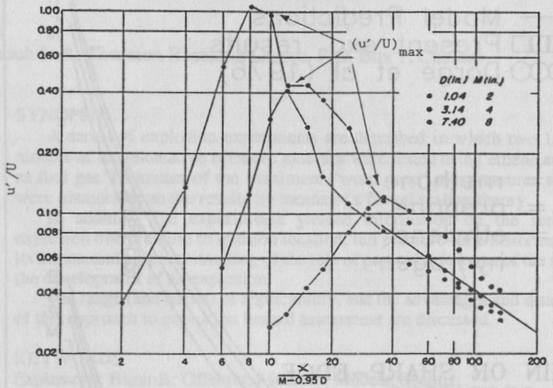

Fig. 6. Intensity of turbulence generated by perforated plates as a function of the normalised downstream distance. (from Baines and Peterson (29)).

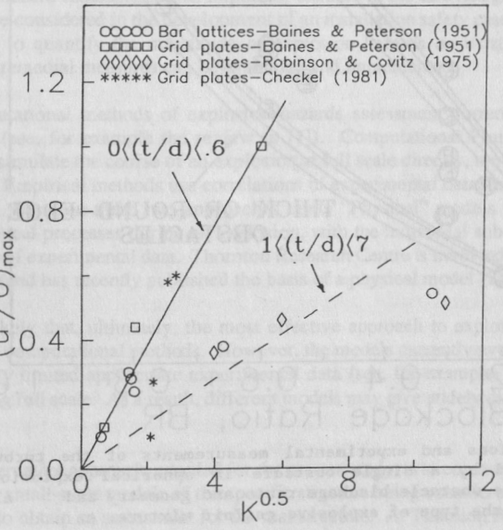

Fig. 7. Correlation of the maximum tubulence intesnsity generated by an obstacle as function of the pressure loss coefficient and the aspect ratio (t/d) of the obstacle.

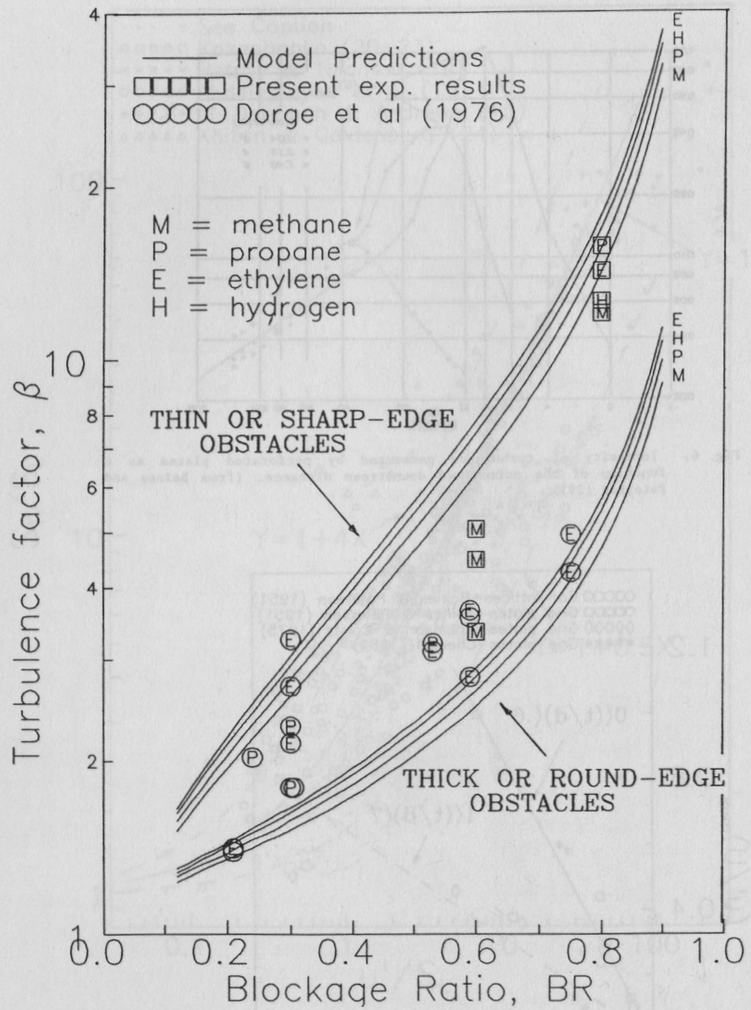

Fig. 8. Model predictions and experimental measurements of the turbulence factor induced by a single obstacle in spherical explosions as function of the obstacle blackage ratio and geometry and also as a function of the type of explosive gas/air mixture.

EXPLOSION HAZARD ASSESSMENT OF OFFSHORE MODULES USING 1/12th SCALE MODELS

B. Samuels
Shell Research Ltd., Thornton Research Centre, P.O. Box 1, Chester

SYNOPSIS

A series of explosion experiments are described in which two 1/12th scale models of representative offshore modules were tested using ethene and propane as fuel gas. Estimates of the maximum "worst case" overpressures at full scale were obtained from the results by means of a fractal scaling theory.

In addition, the experiments yielded information on the sensitivity of explosion overpressure to ignition location, full pressure-time histories at specific locations, and an understanding of the role of particular features of the structure in the development of an explosion.

The range (and limits) of applicability, and the advantages and disadvantages, of this approach to explosion hazard assessment are discussed.

KEYWORDS
Explosions; Hazards; Offshore Modules; Models; Scaling;

1. INTRODUCTION

Explosion hazard assessment is an important element in the safe design of new offshore platforms, and must be considered in the development of an installation safety case. In addition, it is important to be able to quantify the magnitude of explosion hazards on existing installations, so that, if necessary, remedial measures can be evaluated and implemented.

Computational methods of explosion hazards assessment currently available fall into three categories (see, for example the review in [1]). Computational Fluid Dynamic (CFD) methods attempt to simulate the course of an explosion at full scale directly, requiring substantial computing resources. Empirical methods use correlations of experimental datasets to attempt to extrapolate to real cases. Between these two approaches come "Physical" models that attempt to describe the global physical processes during an explosion, with the individual sub-models calibrated against a wide range of experimental data. Thornton Research Centre is involved in developments in all three categories (and has recently published the basis of a physical model [2]).

It is likely that, ultimately, the most effective approach to explosion hazard assessment will come from computational methods. However, the models currently available have only been tested against very limited appropriate experimental data (see, for example, [3]), especially at anything approaching full scale. As a result, different models may give widely differing answers for the same geometry.

An alternative approach, adopted for the present study, is to conduct experimental explosions in (relatively) small-scale models of the specific structure being considered. The results must then be scaled up, to obtain an assessment for the real structure. At Thornton Research Centre, this is done using a fractal scaling theory developed by Taylor and Hirst [4].